Paper:

Artificial Neural Network Based Step-Length Prediction Using Ultrasonic Sensors from Simulation to Implementation in Shoe-Type Measurement Device

Romy Budhi Widodo[*,**] **and Chikamune Wada**[*]

[*]Graduate School of Life Science and Systems Engineering, Kyushu Institute of Technology
2-4 Hibikino, Wakamatsu-ku, Kitakyushu, Fukuoka 808-0196, Japan
E-mail: {romy-budhi@edu., wada@}brain.kyutech.ac.jp
[**]Informatics Engineering Study Program, Ma Chung University
Villa Puncak Tidar N-1, Malang 65151, Indonesia
E-mail: romy.budhi@machung.ac.id
[Received September 1, 2016; accepted November 15, 2016]

Step-length measurement as a spatial gait parameter is useful for the physician and physical therapist for determining the patient's gait condition. We hypothesized that this could be determined using ultrasonic sensors mounted on a shoe-type measurement device. For that purpose, we have developed a shoe-type measurement device to measure gait parameters. Our system was found to effectively measure step-length and pressure distribution. However, we found that the presence of shoes leads to perishable and fragile conditions for the sensors. Therefore, we redesigned the number, angle, and range of the ultrasonic sensors mounted on the shoes in order to clarify and improve the step-length prediction. This paper discusses the improvement of a shoe-type measurement device from the implementation with real shoes and the step-length prediction using an artificial neural network (ANN). The results of the experiment show that the number, angle, and positioning of ultrasonic sensors affect their ability to capture the human step region, that is, 50×70 cm under the experimental condition of foot progression angle up to 30 degrees. The results of the predictive performance of step-length using the proposed ANN architecture demonstrate an improvement.

Keywords: step-length, prediction, applied neural network, shoe-type measurement device, ultrasonic

1. Introduction

The goals of this study were as follows: (1) to implement the simulation results on an actual shoe-type measurement device and evaluate the measurement scope based on the results of previous simulations in our previous study; and (2) to establish a method of processing the distance data from ultrasonic receivers to predict the step-length of human steps using an artificial neural network (ANN). The step-length is the distance between corresponding successive points of heel contact of the opposing feet.

Recently, an increasing amount of research has been driven by interests in gait-assessment systems [1, 2]. Some researchers use an inertial measurement unit (IMU) to measure stride length, an important spatial gait parameter, by processing temporal data [1]. Our previous shoe-type measurement device is for measuring gait performance such as step-length, step width, pressure distribution [3, 4], and attitude estimation during the swing phase using IMU [5], as shown in **Fig. 1**. The previously designed shoe contains ultrasonic receivers and transmitters, pressure sensors, and IMU; it uses seven ultrasonic transmitters and twelve receivers. The sensors are perishable and fragile, so the measurement of gait parameters is prone to error. In order to streamline the sensors and reduce their number, the simulation technique was designed [6]. In the previous iteration, step-length was measured by integrating the ultrasonic sensors and gyro data using a particle filter algorithm.

In order to improve this device's performance, the simulation technique has been designed for our new shoe-type measurement device [6], the results of which are consist with the number of ultrasonic sensors (Murata ultrasonic sensors MA40S4R/S), the optimal sensor angle, and the sensor's position.

In this paper we introduce the actual implementation of the new shoe-type measurement device, including the scope of the measurement's test. Finally, we discuss the implementation of multi-layer perceptron (MLP) for step-length prediction using data from ultrasonic sensors.

2. Implementation

The simulation results from the previous study [6] are as follows: 1) There was a reduction in the number of ultrasonic transmitters (Tx) and receivers (Rx) from the previous shoe-type measurement device; 2) We found three

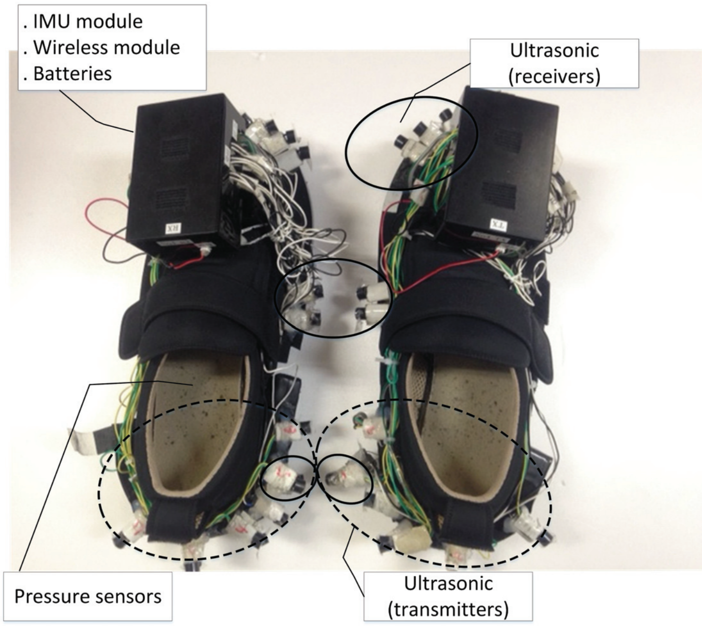

Fig. 1. The previous shoe-type measurement device.

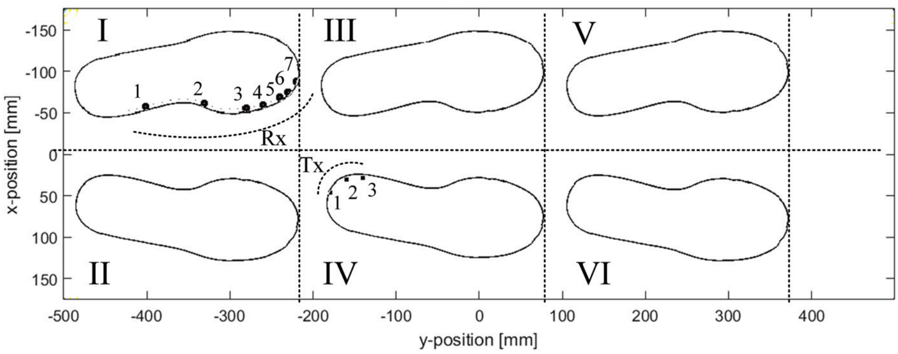

Fig. 2. The final representation of the region division, seven position of ultrasonic receivers (Rx), and three ultrasonic transmitters (Tx); were based on the previous study.

ultrasonic Tx and seven Rx in each shoe as an optimal result, including their position and angle of each Rx based on the maximum acoustic pressure that was received from each Tx as well. An illustration of sensors positions is shown in **Fig. 2**; it indicates the usage of three ultrasonic transmitters and seven ultrasonic receivers in each shoe. The implementation on the actual shoe-type measurement device is shown in **Fig. 3**.

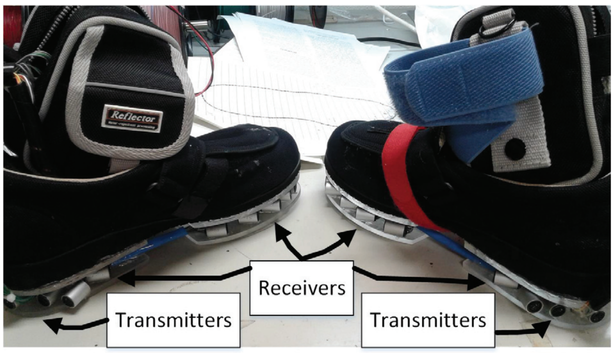

Fig. 3. The implementation of the position and angle of ultrasonic sensors based on the simulation.

2.1. Test Setup and Experimental Design

To verify and validate the results of the simulation, the test was conducted using ultrasonic transmitters (MA40S4S) and ultrasonic receivers (MA40S4R). **Table 1** lists the specifications of ultrasonic sensors that come from Murata Co., Ltd., Japan. We used a plan board and made a 50×70 cm grid system, which is the grid size 10×10 cm as illustrated in **Fig. 4**.

The width of the board is determined based on the distance between two heels (walking base) for an average person, that is, 5 to 13 cm [7–9]. We implemented it using a 50 cm width of a plan board in order to test the measurement scope of the sensors. The length of the board is determined based on the average length of the adult human step, i.e., half of the stride length, and followed the simulation region. The mean stride length during normal

Table 1. Specification of Murata ultrasonic sensor.

Part Number	MA40S4R/S
Construction	Open structure type
Using method	Receiver and Transmitter (dual use) type
Nominal frequency (kHz)	40
Sound Pressure (dB)	120 ± 3 (20 Pa)
Directivity (deg)	80
Detectable range (m)	0.2–4
Dimension (mm)	$9.9\varnothing \times 7.1$ height
Input voltage (Vp-p)	20 (40 kHz) continuous signal

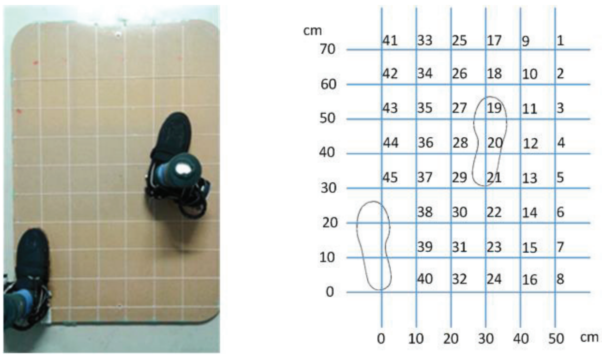

(a) (b)

Fig. 4. Test setup and grid division for data retrieval. (a) the board as a testbed; (b) grid division and grid number 1 to 45.

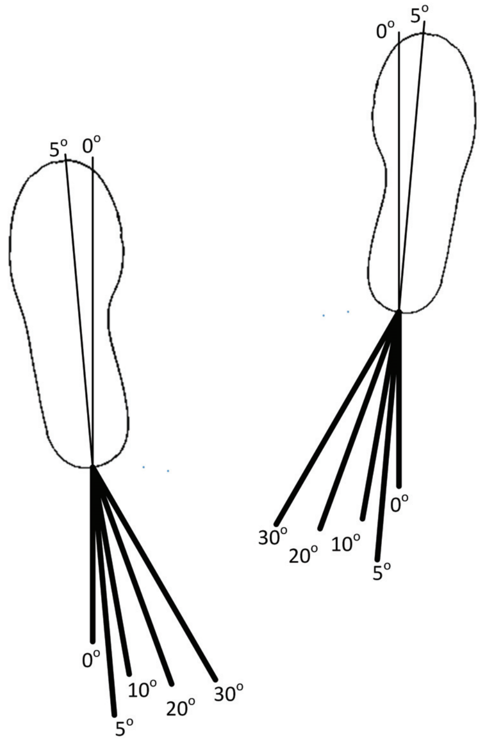

Fig. 5. The combination of left and right foot progression angle during data retrieval. The capturing figure illustrates the 5-degree progression angle.

walking in adults ranges from 0.7 m [8, 10] to 1.3 m [2].

The C# acquisition data were used to collect the distances between ultrasonic transmitters and receivers. The data retrieval in **Fig. 4** was conducted when the left shoe was on the grid $(0,0)$ cm and the right shoe was moved sequentially from the 1^{st} grid to the 45^{th} grid. Assuming that all ultrasonic Tx and Rx are identical between the left and right shoes, we retrieved all data from one side of the human step, in this case, the right step. The positions of ultrasonic Tx and Rx are defined from the results of simulation as shown in **Fig. 2** as well as the implementation as shown in **Fig. 3**. At every point grid, we retrieved the distance between each receiver and transmitter pair from 25 combinations of foot progression angles. The test of the measurement scope used the foot progression angle up to 30 degrees which consists of five steps: 0, 5, 10, 20, and 30 degrees. The 25 combinations came from these five steps of foot progression angles for each shoe. We used a protractor to determine the foot progression angle as shown in **Fig. 5**.

2.2. Measurement of Scope Result

The test of measurement scope at every grid point using 25 shoe angle combinations resulted in almost all grid points with a measurement scope of 100%. This means that in all 25 shoe angle combinations, the distance data between all Tx and Rx pairs are available. However, in grid numbers 7, 8, 15, 16, 24, 32, and 40, we found that data are not available for all shoe angle combinations. In the 8^{th} and 24^{th} grids, the scope of measurement is 48%, whereas on the 16^{th} grid, the scope of measurement is 56%. In the same way, we found that on the 7^{th} grid the measurement scope is 68%, whereas on the 15^{th}, 32^{nd}, and 40^{th} grids, the measurement scope is between 70% and 80%. The remaining grid points show 100% of measurement scope. **Fig. 6** shows the conclusion of the measurement scope.

3. Step-Length Prediction

The step-length is one of the temporal gait parameters measured during the double support phase. We measured the step-length between the two heels of the left and right foot. In a pathological gait, it is possible that the two-step length is different; therefore, the step-length is one of the important gait parameters for clinical gait analysis.

The ultrasonic waves commonly display nonlinear propagation behavior due to the influence of angle direction and the relatively high amplitude to wavelength ratio. The measurement of distances between each pair of receivers and transmitters in our implementation in the previous section shows the tendency of unsteady value. In this case, a heuristic technique that can learn from the situation and provide results through intelligent guesswork is needed. The ANN has the ability to learn through training and provide results by generalizing broad categories from specific examples.

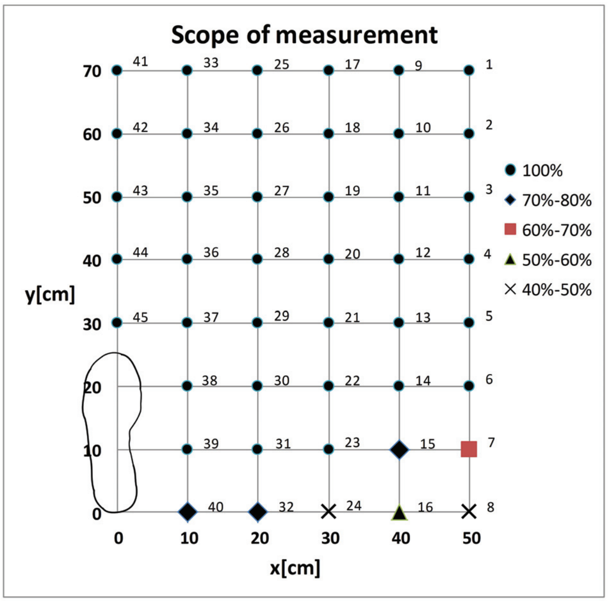

Fig. 6. Final result of the measurement scope of ultrasound Tx-Rx pairs.

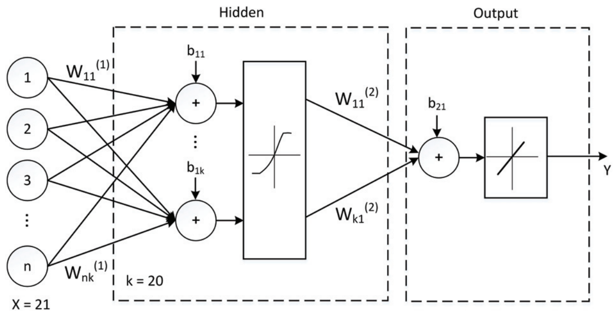

Fig. 7. Network type A: two-layer neural network with hyperbolic tangent sigmoid and linear transfer function: X input corresponds to the number of data pair between ultrasonic Tx-Rx, W-weights from input layer to hidden layer and from hidden layer to output layer, b-biases of the neurons in hidden and output layer.

3.1. Data Preparation During the Development of ANN

At each grid point, we performed 25 combinations of the foot progression angle; for each combination angle, we retrieved 300 points of data. Therefore, we have 7500 points of data for each grid point for one pair of Tx-Rx. Therefore, having 21 pairs of Tx-Rx, we have a total of 21×7500 of measurement data points for each grid point. In the beginning, the total grid point was 45, as shown in **Fig. 4(b)**; therefore, we have 21×337500 data points. By observing the data, we found that some grids, as described in the previous section, are out of the measurement scope; therefore, we assume some of those data to be noise for the learning process in ANN. Although the learning process in the network can handle noise in the training data, too many erroneous training values may prevent the ANN from learning the desired model [11]. The filtered data now become 21×330600 from 21×337500 previously. The data will be divided randomly into three parts of samples within its proportion as follows: training (70%), validation (15%), and testing (15%). The 21 pairs of measurements between ultrasonic Tx and Rx were used as input to the ANN for training, validation, and testing.

The ANN output is based on its architecture type. The type A network output comes from the Euclidean distance between the positions of the left shoe's heel and the right shoe's heel. For example, the distance between coordinate $(0,0)$ to the 27^{th} grid point, for which the coordinate is $(20,50)$, is 53.85 cm (refer to **Fig. 4(b)** for the grid numbers). On the other side, the output of the type B network is designed to be a multiplier coefficient for the actual step-length output, to be described in detail in the next subsection.

3.2. Network Architecture and Training Algorithm

We focus on a multilayer network rather than a single layer or recurrent network. The network is a two-layer neural network, the purpose of which is two-stage regression [12]. For regression, typically the number of nodes in the output layer is one [12]; however, in common the multiple nodes in the output layer can handle multiple quantitative responses. In accordance with these statements, two different suggestions for networks will be considered, as follows: a two-layer network with 1 node in the output layer (network A), and a two-layer network with 45 nodes in the output layer (network B). The parameters of the type A network are: (1) 21 input nodes, (2) 20 neurons in the hidden layer, (3) 1 output node, (4) the required training error (mse) $= 0.1$, (5) 1000 training epochs, and (6) the maximum failures of validation check $= 6$. The total of learnable parameters (weights and biases) is 461 parameters. The one output node represents the Euclidean distance in linear representation. The stopping criteria were the training error, the number of epochs, or the maximum validation failures. We found that by using 20 neurons in the hidden layer, the number of training epochs was exceeded, and the validation checks never exceeded the maximum limit. When a small number of neurons were used, we noticed that the maximum failure of the validation checks occurred before 1000 epochs elapsed. **Fig. 7** represents the type A network.

Regarding network B, the parameters are as follows: (1) 21 input nodes, (2) 20 neurons in the hidden layer, (3) 45 output nodes, (4) the required training error (mse) $= 0.015$, (5) 1000 training epochs, and (6) the maximum failures of validation check $= 6$. During training, it was observed that after 200 epochs, the mse requirement was fulfilled. The difference between network A and network B parameter settings is on the required mse; this is because the output target is different for both networks. The 45 output nodes represent 45 grids as in the simulation design. The value of 0 or 1 was used in the output training data. The result of the network will be recognized as the multiplier coefficient (y_i), therefore the sum of all multiplication between each output node and its related

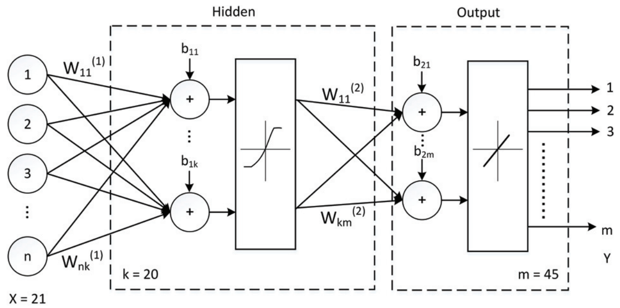

Fig. 8. Network type B: two-layer neural network with 45 output nodes.

Euclidean distance (E_i) on that node is the real output of the network (Y), as in Eq. (1). **Fig. 8** shows the type B network.

$$Y = \sum_{i=1}^{45} y_i E_i \quad . . . . (1)$$

The training process in the ANN has the purpose of updating the weight value in the connection between neurons. Many training algorithms have been found in the process of finding the minima in error space and speeding up the convergence. The multilayer network in this study was trained using the Levenberg-Marquardt (LM) algorithm. The LM algorithm blends the steepest descent method (error back-propagation) and the Gauss-Newton algorithm [13]. The LM algorithm integrates the speed advantage of the Gauss-Newton algorithm and the steepest descent's stability. It works by switching mechanisms; around the area with complex curvature, the LM algorithm uses the steepest descent algorithm; when the curvature is adequate to make a quadratic approximation, the LM algorithm uses the Gauss-Newton algorithm to speed up the convergence. In [13] it is shown that the Levenberg-Marquardt algorithm is stable and fast, it surpasses the steepest descent algorithm, the Newton algorithm, and the Gauss-Newton algorithm.

The transfer function for the hidden layer is a hyperbolic tangent sigmoid, which compresses real numbers to range from $[-1,1]$, while the transfer function in the output layer is linear.

3.3. Setup for the Experiment and Results

3.3.1. Setup and Condition for the Experiment

The MATLAB® program was used to execute the ANN training process and output calculation using network types A and B. The reliability test for those networks was also conducted using a MATLAB® program. The sensor data acquisition from ultrasonic receivers was made using C# program. The sampling rate for ultrasonic sensors and pressure sensor boards is 30 Hz in the specification of the controller as suggested in [14]; however, finally we got 26 Hz as final sampling rate due to the numbers of ultrasonic sensors and pressure sensors. To verify and validate the prediction of the step-length, we conducted a walking experiment using a shoe-type measurement device; the weight of the shoe was 1.2 kg including ultrasonic sensors, pressure sensors inside the insole board, IMU sensor, controller unit, wireless unit, and batteries. For a reference measurement, the measurement setup contained six OptiTrack® cameras as shown in **Fig. 9(a)**. Reflective markers were placed on the heels in order to measure distance during walking as shown in **Fig. 9(b)**.

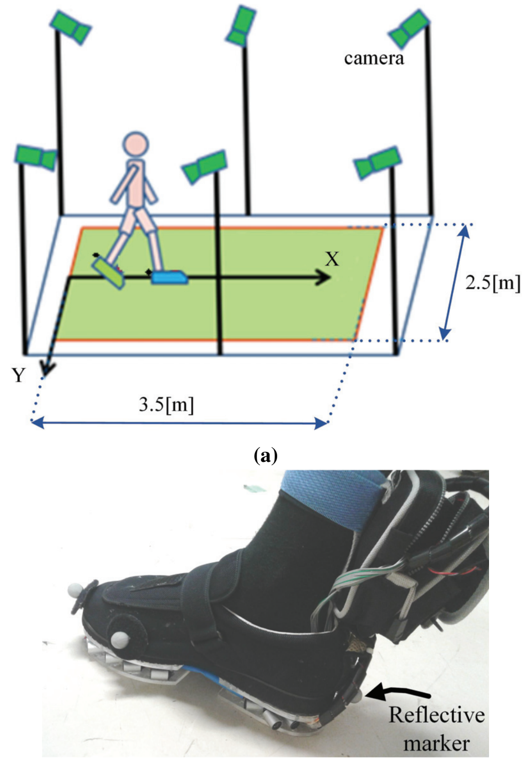

Fig. 9. Measurement setup: (a) room setup for recording the markers distance; (b) Shoe-type measurement device with reflective markers.

Table 2. The experiment condition.

Parameter	Value
Gait speed	0.266 m/s
Cadence	21 strides/min
Stance phase time	0.73 s

The experiment of walking as explained in the next subsection was conducted as a slow-walking type, using some observable conditions such as gait speed, cadence, and stance phase time, is described in **Table 2**. The measurement of gait speed comes from the average of time divided by distance; time elapsed within the specific distance comes from motion-capturing time framing, whereas the distance comes from the difference between the finish and the start position of each walking task. The measurement of cadence comes from the definition that cadence (strides/min) is calculated by dividing 60 seconds by a stride time (seconds) [15]. The measurement of stance phase time comes from gyro ($\pm$1500 deg/s) (Logical Product Co. Ltd., Japan); the stance time was mea-

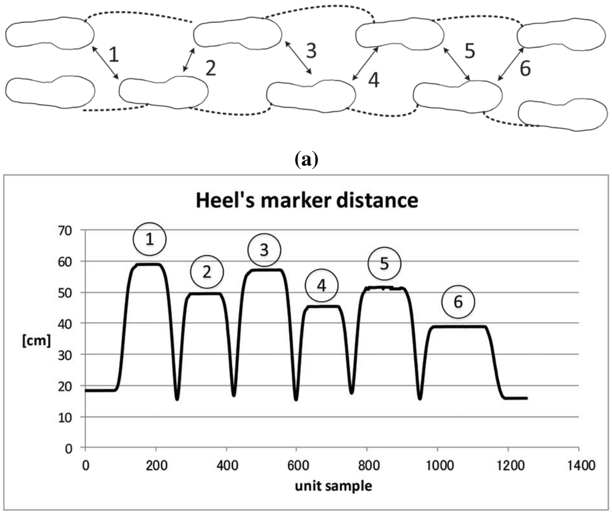

(a)

(b)

Fig. 10. The illustration of one task of walking experiment: (a) One task of experiment consist of 3–4 steps of each foot (the two-headed arrow indicates the step-length). (b) The distance between two heels as a reference measurement from motion captures system.

sured when the *y*-axis of gyro signal under the specific threshold indicated that there is no foot movement; in this case, we heuristically use 10 deg/s as a threshold and the *y*-axis is the plantarflexion-dorsiflexion axis.

3.3.2. Results of the Experiment

The first result is the training process for the networks. Network A took 55 minutes for the training process after 1000 epochs. As the learnable parameter number for network B is larger than that for network A, the training process for network B took 77 hours, and the performance *mse* of 0.015 was reached after 200 epochs.

After finishing the training process for network A and network B, we conducted the reliability test to ensure that those networks were able to fit in all the data. The reliability test data were chosen from trained and untrained data, and the performance was measured using *rmse* (root mean square error). The result for network A indicates that the difference of *rmse* between trained and untrained data is 3.86%, while in network B, the *rmse* difference between trained and untrained is 0.83%.

The actual implementation experiment is the walking task. This experiment is derived from the average of six walking tasks. In each task of the walking experiment, we collected 3-4 steps from each foot. There are a total of 37 steps in this experiment, consisting of 19 right steps and 18 left steps. **Fig. 10** shows an example of one task in the walking experiment. In **Fig. 10(a)**, the marked numbers 1 to 6 indicate that there are six instances of step-length measurement. The corresponding distance between the markers on the heels is shown in **Fig. 10(b)** by the motion-capturing measurement system. Overall, the detailed experiment results and the performance of step-length prediction between network A and network B compared to the reference are shown in **Table 3**.

We also compared the results of the step-length prediction from the previous study when using the integration of gyro and ultrasonic sensors in the particle filter algorithm [3, 4]. The second comparison is from the work of B. Mariani, et al. [1] with the prediction of stride length using temporal IMU data. In the third comparison of prediction using 5 Hz differential GPS (DGPS) as in [16], the step-length error was calculated using step duration (0.53 ± 0.01 s) times the speed error per step (0.8 cm/s), which is 0.42 cm in the results. **Table 4** shows the comparison results between ANN, particle filter, temporal IMU data, and DGPS.

4. Discussion and Limitations of the Experiment

4.1. Discussion

The result of the simulation has been concluded in **Fig. 2**, resulting in seven ultrasonic receivers and three ultrasonic transmitters. Using these sensors, the number and its angle; the implementation has been conducted as shown in **Fig. 3**. A test bed of 50×70 cm board area was used in the implementation. The result of the measurement scope in **Fig. 6** shows some blank areas when the shoe position is on the straight line, for example, the left shoe on the coordinate $(0,0)$ and the right shoe either on the $(10,0)$, $(20,0)$, $(30,0)$, $(40,0)$, or $(50,0)$. This result was in line with the simulation design that the normal human steps fall either in the region IV or region VI. The straight-line position of two feet in the frontal axis is not found in normal walking. The distance between all ultrasonic receivers and transmitters was detected well until the coordinate of $(50,70)$ or grid number 1, as shown in **Fig. 6**; this shows that the distance between two feet of the normal human step can be detected using this system.

In the simulation the foot progression angle that was used is 10 degrees because the normal foot progression angle is 8–12 degrees [17]. The implementation result shows that up to 30 degrees of foot progression angle, the system still works well.

Comparing the training process between network A and network B, it was found that the type A network has a shorter training time and a smaller mean absolute error for all foot step than network B. Network B has more learning parameters to be updated in each epoch and showed that it needed to be standardized by Eq. (1). By using the reliability test, both types of networks were shown to be able to make prediction generalizations. The differences in *rmse* between the untrained and trained data in both networks were below 5%. In regard to reliability, both networks are ready to be used for the shoe-type measurement device. Observing **Table 3**, it can be seen that network A has a better performance than network B in the left step, right step, and also in all step criteria. Finally, network A was chosen due to its efficacy.

By using our combined data from ultrasonic trans-

Table 3. The result of walking task experiment in details and a comparison between networks A and B; mean absolute error is presented as mean (standard deviation) with all data in *cm*.

	Network A			**Network B**		
	Reference (cm)	Prediction (cm)	error (cm)	Reference (cm)	Prediction (cm)	error (cm)
Right step	58.95	56.77	2.18	58.95	56.13	2.82
	57.19	55.33	1.86	57.19	55.62	1.57
	51.64	49.6	2.04	51.64	49.54	2.1
	51.4	50.15	1.25	51.4	49.8	1.6
	47.61	44.97	2.64	47.61	43.9	3.71
	50.45	49.37	1.08	50.45	49.82	0.63
	49.16	47.34	1.82	49.16	48.4	0.76
	50.3	48.05	2.25	50.3	47.2	3.1
	31.36	30.82	0.54	31.36	29.62	1.74
	47.71	45.42	2.29	47.71	43.49	4.22
	45.21	43.45	1.76	45.21	42.22	2.99
	47.23	45.78	1.45	47.23	43.66	3.57
	32.5	31.84	0.66	32.5	29.71	2.79
	38.93	36.73	2.2	38.93	40.92	1.99
	44.13	44.75	0.62	44.13	42.83	1.3
	39.42	37.2	2.22	39.42	41.11	1.69
	42.94	41.11	1.83	42.94	42.08	0.86
	37.33	35.56	1.77	37.33	41.73	4.4
	45.67	43.45	2.22	45.67	43.31	2.36
	Mean absolute error (sd)		1.72 (0.6)	Mean absolute error (sd)		2.33 (1.11)
Left step	49.53	47.83	1.7	49.53	44.7	4.83
	45.45	44.23	1.22	45.45	42.34	3.11
	38.93	35.14	3.79	38.93	32.94	5.99
	44.45	42.75	1.7	44.45	42.11	2.34
	46.83	43.99	2.84	46.83	40.55	6.28
	44.97	43.07	1.9	44.97	42.49	2.48
	44.9	42.94	1.96	44.9	42.12	2.78
	46.2	44.28	1.92	46.2	43.16	3.04
	39.57	35.94	3.63	39.57	35.01	4.56
	40.35	38.35	2	40.35	37.32	3.03
	43.51	41.73	1.78	43.51	41.81	1.7
	46.78	44.86	1.92	46.78	42.25	4.53
	43.46	45.02	1.56	43.46	36.77	6.69
	43.7	38.16	5.54	43.7	32.29	11.41
	44.45	41.67	2.78	44.45	45.6	1.15
	36.55	32.55	4	36.55	30.78	5.77
	39.94	36.62	3.32	39.94	33.12	6.82
	46.59	39.11	7.48	46.59	37.81	8.78
	Mean absolute error (sd)		2.84 (1.56)	Mean absolute error (sd)		4.74 (2.57)
Mean absolute error (sd) of all steps	Network A		2.26 (1.3)	Network B		3.50 (2.3)

mitters and receivers as inputs and by choosing the Levenberg-Marquardt algorithm as a training function, we were able to solve our problem in step-length prediction. The error of the prediction as concluded in **Table 3** indicates that the error of the left step is larger than the error in the right step. We presume that between the left and right shoe, the position and angle of sensors is not exactly identical; this is due to the manual construction or handmade construction. Since the training data come from one side of the step, that is, the right step; so we found that the prediction performance of the right step surpasses the performance of the left step. This is also a remarkably counsel for our experience in using artificial neural networks for solving the shoe-type measurement device problems in future study.

Table 4. The comparison of average error of step-length prediction using four different methods; presented as average (standard deviation) with all data in *cm*.

Methods	Average error
ANN	2.26 (1.3)
Particle filter	4.00 (2.0)
Inertial sensor	1.50 (6.8)
DGPS	0.42 (0.01)

The comparison study of the step-length prediction has been shown in **Table 4**. At a glance, the prediction using DGPS by P. Terrier, et al. [15] surpasses other methods. However, GPS has shortcomings such as the high cost of professional equipment and is recommended only for outdoor analysis. The second-best prediction performance was proposed using inertial sensor by B. Mariani, et al. [1]. However, the complexity of inertial sensor data processing and additional computational time might be one of the reasons to choose the ultrasonic sensor and ANN as a processing method for the shoe-type measurement device. Using the same kind of sensor as inputs, the ANN method surpasses the particle filter method; however, we do not claim that this condition is a global case, as many factors might influence reducing the particle filter method, such as the synchronization with gyro data as in [3], the difference of experimental conditions, and the number of sensors used.

4.2. Limitations

The results of the simulation [6] and implementation have succeeded in determining the position and angle of ultrasonic sensors. Likewise, the step-length prediction results showed an improvement of performance from the previous study. From these results, we were able to ensure that the mechanism of simulation, implementation, and ANN architecture design have the influence to improve our shoe-type measurement device. Despite these improvements, there are several major limitations of the experiment that are described below.

The first limitation of the experiment is in the area of its scope. In this study, we used a 50×70 cm board based on a normal human walking area. In addition, we used the 30 degrees of maximum foot progression angle (out-toeing). However, in the case of some gait impairments due to disease or injury, the foot progression angle is possibly in-toeing; it is also possibly that the walking base is more than 50 cm. For the time being, the shoe-type measurement system is suitable for a normal gait.

The second limitation is the design position of the ultrasonic transmitter on the medial heel of both feet with a 60-degree azimuth angle. This position, despite its efficacy to measure the distance on the range of the human step, has its flaws. It cannot precisely measure the distance between the two heels when the position of the foot is in a straight line of frontal axis to the body. This has been shown in **Fig. 6** on grid numbers 8, 16, 24, 32, and 40.

The third limitation is related to the use of an artificial neural network as the two-stage regression. The step-length prediction using an artificial neural network has its flaws. One problem is that the ANN is like a black box; i.e., the mathematic model of the prediction cannot be defined. Another problem is that we cannot know which the final network is the best overall; it depends on the initial weight and biases in every training process.

The fourth limitation is related to experiment conditions; as shown in **Table 2**, we used a slow speed of walking in this experiment. In the future, both normal speeds and fast speeds will be considered. Also, in this paper, we do not integrate each joint movement of the lower extremities and trunk as well as the analysis of plantar pressure. As a future work, the integration of body link model and sensors' measurement will be considered in order to analyze complete gait.

5. Conclusion

One of the main contributions of this paper is the validation of the measurement scope of step-length by implementing the simulation result as an actual shoe-type measurement device. The range of the human step and foot progression angle were successfully cope using the number of sensors and its angle based on the actual measurement; the results of implementation have been concluded in **Fig. 6** as the measurement scope diagram.

One of the real-world applications already mentioned as an objective is the prediction of step-length. By using our shoe-type measurement device, the prediction of human step-length can be achieved by implementing an artificial neural network to solve the nonlinearity of ultrasonic data. Despite the efficiency of the method, it still has its flaws; the step-length prediction error of the human walking experiment has been shown in **Table 3**. Nevertheless, as a future problem to be solved, we hypothesized that another spatial parameter of gait such as foot progression angle is possible to predict using these ultrasonic receivers' data.

Acknowledgements

R. B. Widodo would like to thank his colleagues in the Informatics study program at Ma Chung University for servings as peers during the prediction design. The authors would like to thank all those who served as volunteers.

References:

[1] B. Mariani, C. Hoskovec, S. Rochat, C. Büla, J. Penders, and K. Aminian, "3D gait assessment in young and elderly subjects using foot-worn inertial sensors," J. of Biomechanics, Vol.43, pp. 2999-3006, 2010.

[2] F. Dadashi, B. Mariani, S. Rochat, C. J. Büla, B. Santos-Eggimann, and K. Aminian, "Gait and foot clearance parameters obtained using shoe-worn inertial sensors in a large-population sample of older adults," Sensors, Vol.14, pp. 443-457, 2014.

[3] C. Wada, F. Wada, K. Hachisuka, T. Ienaga, Y. Kimuro, and T. Tsuji, "Improvement study for measurement accuracy on wireless shoe-type measurement device to support walking rehabilitation," Proc. of Int. Conf. on Complex Medical Engineering, pp. 471-474, 2012.

[4] S. Ikeda and C. Wada, "Estimation of foot placement during walking by particle filter method," The 28th Symposia of SICE Sensing Forum Measurement Division, pp. 105-108, 2011 (in Japanese).

[5] R. B. Widodo and C. Wada, "Attitude Estimation Using Kalman Filtering: External Acceleration Compensation Considerations," J. of Sensors, Vol.2016, Article ID 6943040, p. 24, 2016, doi:10.1155/2016/6943040.

[6] R. B. Widodo and C. Wada, "Simulation of Ultrasonic Sensors in a Shoe-Type Measurement Device," Proc. of the SICE Annual Conf., pp. 1490-1493, 2016.

[7] C. Kirtley, "Clinical Gait Analysis: Theory and Practice," Elsevier Churchill Livingstone, China, 2006.

[8] D. J. Magee, "Orthopedic Physical Assessment," 6th edition, Elsevier Saunders Canada, 2014.

[9] D. Levine, J. Richards, and M. W. Whittle, "Gait Analysis," 5th edition, Elsevier Churchill Livingstone, China, 2012.

[10] B. Abernethy, V. Kippers, S. J. Hanrahan, M. G. Pandy, A. M. McManus, and L. Mackinnon, "Biophysical Foundations of Human Movement," 3rd edition, Human Kinetics, Macmillan Education, Australia, 2013.

[11] S. Walczak and N. Cerpa, "Heuristic principles for the design of artificial neural networks," Information and Software Technology," Vol.41, pp. 107-117, 1999.

[12] T. Hastie, R. Tibshirani, and J. Friedman, "The Elements of Statistical Learning: Data Mining, Inference, and Prediction," 2nd edition, Springer, 2008.

[13] H. Yu and B. M. Wilamowski, "Levenberg-Marquardt Training," Industrial Electronics Handbook, Vol.5 Intelligent Systems, 2nd edition, Chapter 12, pp. 12-1 to 12-15, CRC Press, 2011.

[14] E. K. Antonsson and R. W. Mann, "The Frequency Content of Gait," J. of Biomechanics, Vol.18, No.1, pp. 39-47, 1985.

[15] R. Tanawongsuwan and A. Bobick, "A Study of Human Gaits Across Different Speeds," Georgia Institute of Technology, Atlanta, 2003.

[16] P. Terrier, Q. Ladetto, B. Merminod, and Y. Schutz, "High-precision Satellite Positioning System as a New Tool to Study the Biomechanics of Human Locomotion," J. of Biomechanics, Vol.33, Issue 12, pp. 1717-1722, ISSN 0021-9290, 2000.

[17] M. D. Bracker and W. J. Wooten, "Musculoskeletal Problems in Children," Family Medicine: Principles and practice, Robert B. Taylor (editor), Vol.1, 5th edition, Springer-Verlag, New York, Inc., 1998.

Name:
Romy Budhi Widodo

Affiliation:
Ph.D. Student, Life Science and Systems Engineering, Kyushu Institute of Technology
Lecturer, Ma Chung University

Address:
2-4 Hibikino, Wakamatsu-ku, Kitakyushu 808-0196, Japan

Brief Biographical History:
1999- Lecturer, Merdeka University
2007- Lecturer, Ma Chung University
2011- Joined Graduate School of IPS, Waseda University
2014- Joined Graduate School of Life Science and Systems Engineering, Kyushu Institute of Technology

Main Works:
• R. B. Widodo and C. Wada, "Attitude Estimation Using Kalman Filtering: External Acceleration Compensation Considerations," J. of Sensors, Vol.2016, Article ID 6943040, p. 24, 2016, doi:10.1155/2016/6943040, http://dx.doi.org/10.1155/2016/6943040.

Membership in Academic Societies:
• The Institute of Electrical and Electronics Engineers (IEEE)

Name:
Chikamune Wada

Affiliation:
Graduate School of Life Science and Systems Engineering, Kyushu Institute of Technology

Address:
2-4 Hibikino, Wakamatsu-ku, Kitakyushu 808-0196, Japan

Brief Biographical History:
1996- Assistant Professor, Research Institute for Electronic Science, Hokkaido University
2001- Associate Professor, Graduate School of Life Science and Systems Engineering, Kyushu Institute of Technology
2016- Professor, Graduate School of Life Science and Systems Engineering, Kyushu Institute of Technology

Main Works:
• "Analysis of Crutch Position in the Horizontal Plane to confirm the stability of the axillary pad for safe double-crutch walking," J. of Physical Therapy Science, Vol.28, No.5, pp. 1438-1442, 2016.
• "Pressure Sensor: State of the Art, Design, and Application for Robotic Hand," J. of Sensors, Article ID:846487, p. 12, 2014.
• "Basic Research on the Method of Presenting Distance Information to the Blind by Means of Gait Measurement," J. of Medical and Biological Engineering, Vol.31, No.4, pp. 283-287, 2011.

Membership in Academic Societies:
• The Institute of Electronics, Information and Communication Engineers (IEICE)
• Japan Ergonomics Society (JES)
• The Institute of Electrical and Electronics Engineers (IEEE)